Modulators of proteostasis: therapeutic targets and diagnostic markers to halt and reverse atrial fibrillation

Marion, D.M.S.

2021

document version
Publisher's PDF, also known as Version of record

Chapter 8

Heat shock protein inducer GGA*-59 reverses contractile and structural remodeling via restoration of the microtubule network in experimental atrial fibrillation

Xu Hu[1], Jin Li[1], Denise M. S. van Marion[1], Deli Zhang[1], Bianca J. J. M. Brundel[1]

[1]Department of Physiology, Amsterdam UMC, Vrije Universiteit Amsterdam, Amsterdam Cardiovascular Sciences, Amsterdam, The Netherlands

Journal of Molecular and Cellular Cardiology. 2019 Sep; 134:86-97

Keywords: geranylgeranylacetone, HSPB1, microtubule, cardiac troponins, atrial fibrillation

Abstract

Background Atrial fibrillation (AF) is the most common progressive tachyarrhythmia. AF progression is driven by abnormalities in electrical impulse formation and contractile function due to structural remodeling of cardiac tissue. Previous reports indicate that structural remodeling is rooted in derailment of protein homeostasis (proteostasis). Heat shock proteins (HSPs) play a critical role in facilitating proteostasis. Hence, the HSP-inducing compound geranylgeranylacetone (GGA) and its derivatives protect against proteostasis derailment in experimental models for AF. Whether these compounds also accelerate reversibility from structural remodeling in tachypaced cardiomyocytes is unknown.

Objective To investigate whether the potent HSP inducer GGA*-59 restores structural remodeling and contractile dysfunction in tachypaced cardiomyocytes and explore the underlying mechanisms.

Materials and Results HL-1 cardiomyocytes post-treated with GGA*-59 or recombinant HSPB1 (rcHSPB1) revealed increased levels of HSPB1 expression and accelerated recovery from tachypacing (TP)-induced calcium transient (CaT) loss compared to non-treated cardiomyocytes. In addition, protein levels of the microtubule protein (acetylated) α-tubulin, and contractile proteins cardiac troponin I (cTnI) and troponin T (cTnT) were reduced after TP and significantly recovered by GGA*-59 or rcHSPB1 post-treatment. The mRNA levels of α-tubulin encoding genes, but not cardiac troponin genes, were reduced upon TP and during recovery, but significantly enhanced by GGA*-59 and rcHSPB1 post-treatment. In addition, TP increased calpain activity, which remained increased during recovery and GGA*-59 post-treatment. However, HDAC6 activity, which deacetylates α-tubulin resulting in microtubule disruption, was significantly increased after TP and during recovery, but normalized to control levels by GGA*-59 or rcHSPB1 post-treatment in HL-1 cardiomyocytes.

Conclusions Our results imply that the HSP inducer GGA*-59 and recombinant HSPB1 accelerate recovery from TP-induced structural remodeling and contractile dysfunction in HL-1 cardiomyocytes. GGA*-59 increases HSPB1 levels, represses HDAC6 activity and restores contractile protein and microtubule levels after TP, indicating that HSP-induction is an interesting target to accelerate recovery from AF-induced remodeling.

Introduction

AF is the most common tachyarrhythmia, accounting for approximately one-third of hospitalizations for cardiac rhythm disturbances with an annual cost of 13 billion euro in the European Union [1]. Its incidence is age-related and growing alarmingly in the ageing population. With the present trend, almost 30 million North Americans and Europeans will be affected with AF by 2050 [2]. AF progression is associated with increased cardiovascular morbidity and mortality, with stroke, myocardial infarction, and heart failure being the most critical complications [3, 4]. In addition, prevention of AF progression from a recurrent intermittent (paroxysmal) to a (longstanding) persistent rhythm disorder is crucial, as persistent AF patients are more refractory to rhythm control therapy [5]. At present, no effective curative therapy exists. Although ablative therapy initially seemed promising, many patients (40-60%) have AF recurrences and require multiple ablation procedures [6]. Current pharmacological therapy is only moderately effective and its usage is limited by pro-arrhythmia and non-cardiovascular toxicities [7]. Electrical cardioversion is only temporarily effective and AF recurs in up to 87% of the patients [8, 9]. Thus, there is a great need to improve AF therapy. To design new therapies, we need to understand the mechanisms driving AF progression. It was previously discovered that the progressive nature of AF is rooted in AF-induced structural remodeling in cardiomyocytes, including degradation of structural and contractile proteins (myolysis) [10-12]. As structural remodeling promotes persistence of the disease [13-15], it is important to uncover the underlying molecular mechanisms with the aim to identify key modulators involved in the reversibility from remodeling.

Our research group previously demonstrated a prominent role for proteostasis derailment as an underlying mechanism for structural remodeling and AF progression [11, 16, 17]. Proteostasis ensures a balanced cellular protein production, folding and clearance of misfolded and/or damaged proteins [18]. A healthy proteostasis is heavily controlled by heat shock proteins (HSPs). HSPs constitute the cell's frontier system to ensure the production and persistence of functional and correctly folded proteins [19, 20]. HSPs are classified in six subgroups namely HSPA (HSP70), HSPB (small HSPs), HSPC

(HSP90), HSPD/E (chaperonin families HSP60/HSP10), HSPH (HSP110) and DNAJ (HSP40) [19, 21]. In the heart, cardiomyocytes express high levels of specific members of the small HSP family, the HSPBs. These include HSPB1 (HSP27), HSPB5 (or αB-crystallin), HSPB6 (HSP20), HSPB7 (cvHSP) and HSPB8 (HSP22) and are considered to safeguard cardiomyocytes from proteotoxicity by stabilizing the contractile apparatus [16, 17, 22-25].

We previously disclosed that some small HSPs, particularly HSPB1, bind to structural proteins and protect them from degradation by calpain in tachypaced atrial cardiomyocytes and human AF [11, 16, 26]. Moreover, we observed that AF increases HDAC6 activity, which deacetylases α-tubulin resulting in depolymerization and degradation of the microtubule network by calpain. In line, inhibition of HDAC6 prevented deacetylation of α-tubulin and calpain-induced microtubule disruption in tachypaced HL-1 cardiomyocytes and protected against AF induction in a dog model for AF, indicating the importance of an intact microtubule network in AF prevention [12].

In addition, the HSP response gets temporarily activated in patients with short duration of AF, but exhausts when AF persists [11]. Consequently, cardiomyocytes lose defense against structural protein degradation, thereby rendering cardiomyocytes increasingly permissive to structural remodeling and AF.

In line with the observed cardio-protective role of HSPB1 in AF, pharmacological treatment with a non-toxic HSP-inducing compound, geranylgeranylacetone (GGA), was found to protect cardiomyocytes from structural remodeling and AF progression [11, 26, 27]. Recently, our research group identified one potent derivative of GGA, named GGA*-59, to reveal superior protective effects against contractile dysfunction in both tachypaced HL-1 cardiomyocytes and *Drosophila* model systems for AF [28]. Whether GGA*-59 enhances recovery from tachypacing-induced structural and contractile remodeling is unknown.

In the current study, we observe GGA*-59 and recombinant HSPB1 to enhance recovery from tachypacing-induced contractile dysfunction and structural remodeling. GGA*-59 and recombinant HSPB1 act via inhibition of HDAC6 activity, thereby resulting in restoration of (acetylated) α-tubulin levels, and the microtubule network in HL-1 cardiomyocytes.

Materials and Methods

HL-1 atrial cardiomyocyte reversibility model and calcium transient measurements

Information on HL-1 atrial cardiomyocyte culture and description of calcium transient measurements can be found in the supplementary materials and methods section.

GGA*-59 treatment of HL-1 cardiomyocytes

After subjecting HL-1 cardiomyocytes to 10 h TP, the cardiomyocytes were post-treated with 10 µM GGA*-59 (Chaperone Pharma BV, the Netherlands) or the same volume of DMSO for 8 h, followed by various measurements.

Protein isolation and Western blot analysis

HL-1 cardiomyocyte samples were used for protein extraction. Detailed methods are available in the supplementary materials and methods section.

Quantitative RT-PCR

Total RNA was isolated from cardiomyocytes by using the NucleoSpin RNA isolation kit (Machery-Nagel). First strand of cDNA was generated by using the iScript cDNA synthesis kit (BioRad). The relative changes in transcription levels were determined by using CFX384 Real time system C1000 Thermocycler in combination with SYBR green supermix (Biorad) and primers (Invitrogen). The calculations were performed by using comparable threshold cycle method, fold changes were adjusted to GAPDH or β-actin levels. Primer sequences are listed in the supplementary materials and methods section.

Chariot transfection of recombinant HSPB1 in tachypaced HL-1 cardiomyocytes

The transfection of recombinant HSPB1 in HL-1 cardiomyocytes is described in detail in the supplementary materials and methods section.

Calpain activity measurement

The calpain activity was measured in protein extracts of HL-1 cardiomyocytes subjected to various conditions. Detailed methods are available in the supplementary materials and methods section.

Fractionation of depolymerized and polymerized α-tubulin

The fractionation of depolymerized and polymerized α-tubulin was described previously for HL-1 cardiomyocytes. Detailed methods for this study are described in the supplementary materials and methods section.

Immunofluorescent staining

The immunofluorescent staining of the microtubule network was conducted in HL-1 cardiomyocytes. Detailed methods are available in the supplementary materials section.

HDAC6 activity measurement

The HDAC6 activity was measured in protein extracts of HL-1 cardiomyocytes according to the protocol as described in the supplementary materials and methods section.

Statistics analysis

Results were expressed as mean ± SEM of at least duplicated independent experiments. Statistical analysis was performed by using a Student's *t*-test. All *P* values were 2 sided. $P \leq 0.05$ was considered statistically significant. GraphPad Prism 5 was used for all the statistic evaluations.

Results

GGA*-59 post-treatment enhances recovery from calcium transient loss in HL-1 cardiomyocytes

Previously, we observed that tachypacing reduces CaT amplitudes [12, 26, 29, 30]. To test whether reduction in CaT amplitude in HL-1 cardiomyocytes is reversible in a time dependent manner, cardiomyocytes were tachypaced for 10 h, followed by recovery for 8, 16 or 24 h. Tachypacing caused a significant reduction of CaT amplitudes, which persisted after 8, 16 and 24 h recovery (Figure 1A, C). In our previous study, we identified a potent HSP-inducing compound GGA-derivative, GGA*-59, to significantly protect against CaT loss upon tachypacing [28]. In the current study, HL-1 cardiomyocytes were tachypaced for 10 h, followed by post-treatment with GGA*-59 for 8 h or 24 h. Interestingly,

post-treatment with GGA*-59 significantly reversed tachypacing-induced CaT loss after 8 h and 24 h recovery compared to DMSO-treated cardiomyocytes (Figure 1B, D, Figure S2A, B and Figure S3). These findings indicate that the HSP-inducing compound GGA*-59 accelerates recovery from tachypacing-induced CaT loss.

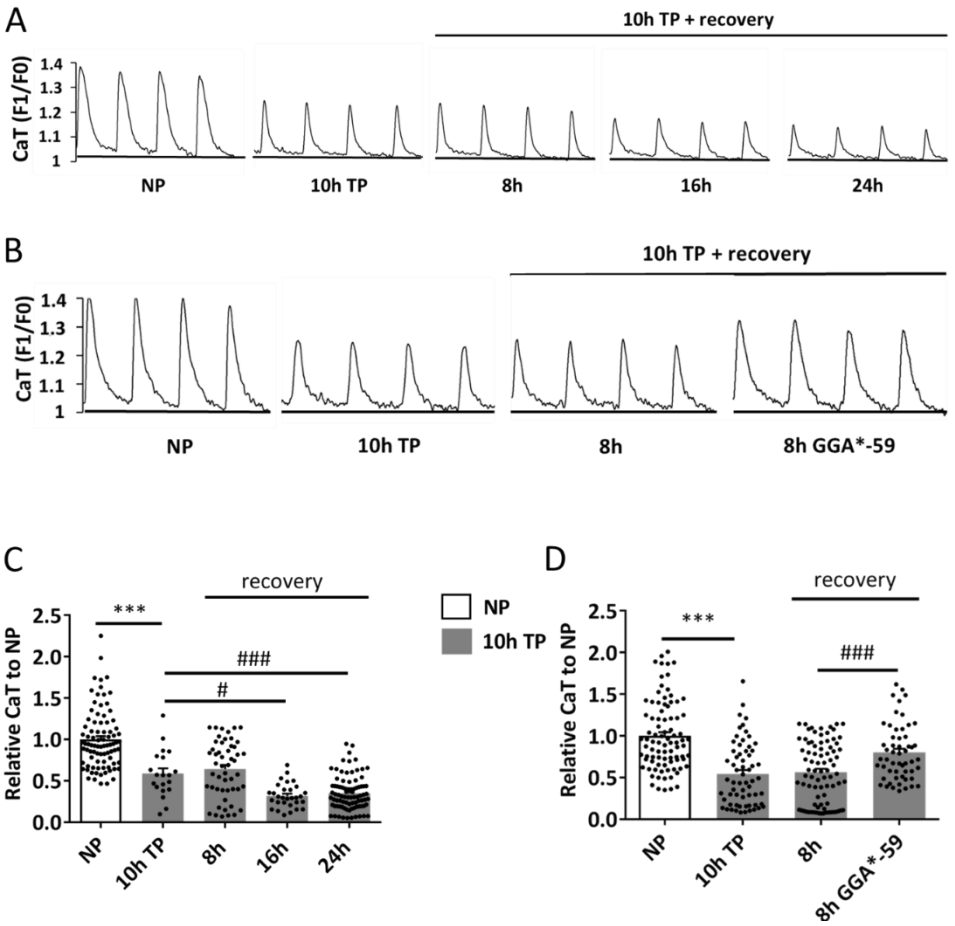

Figure 1. Tachypacing induces persistent CaT loss in HL-1 cardiomyocytes, which is restored by post-treatment with GGA*-59

(**A**) Representative CaT of control non-paced (NP), 10 h tachypaced (TP), and TP followed by 8 h, 16 h or 24 h recovery in HL-1 cardiomyocytes. CaT signals of one cardiomyocyte were measured for 10 s, which generated 10 peaks; 4 peaks were used as the representative tracers. (**B**) Representative CaT of control non-paced (NP), 10 h tachypacing (TP), and TP with 8 h recovery with DMSO-treatment and TP with 8 h post-treatment with 10 µM GGA*-59 during recovery of HL-1 cardiomyocytes. (**C**) Quantified CaT amplitudes (relative to NP) of HL-1 cardiomyocytes showing gradual reduction during recovery from TP. ***P<0.001 vs NP, $^{\#}P$<0.05 and $^{\#\#\#}P$<0.001 vs 10 h TP. N (NP)=86, N (10h TP)=20, N (8h)=51, N (16h)=30, N (24h)=88 cardiomyocytes. (**D**) Quantified CaT amplitudes (relative to NP) of HL-1 cardiomyocytes showing enhanced recovery from CaT loss by GGA*-59 post-treatment. ***P<0.001 vs NP and $^{\#\#\#}P$<0.001 vs 8 h recovery. N (NP)=88, N (10h TP)=63, N (8h)=83, N (8h GGA*-59)=55 cardiomyocytes.

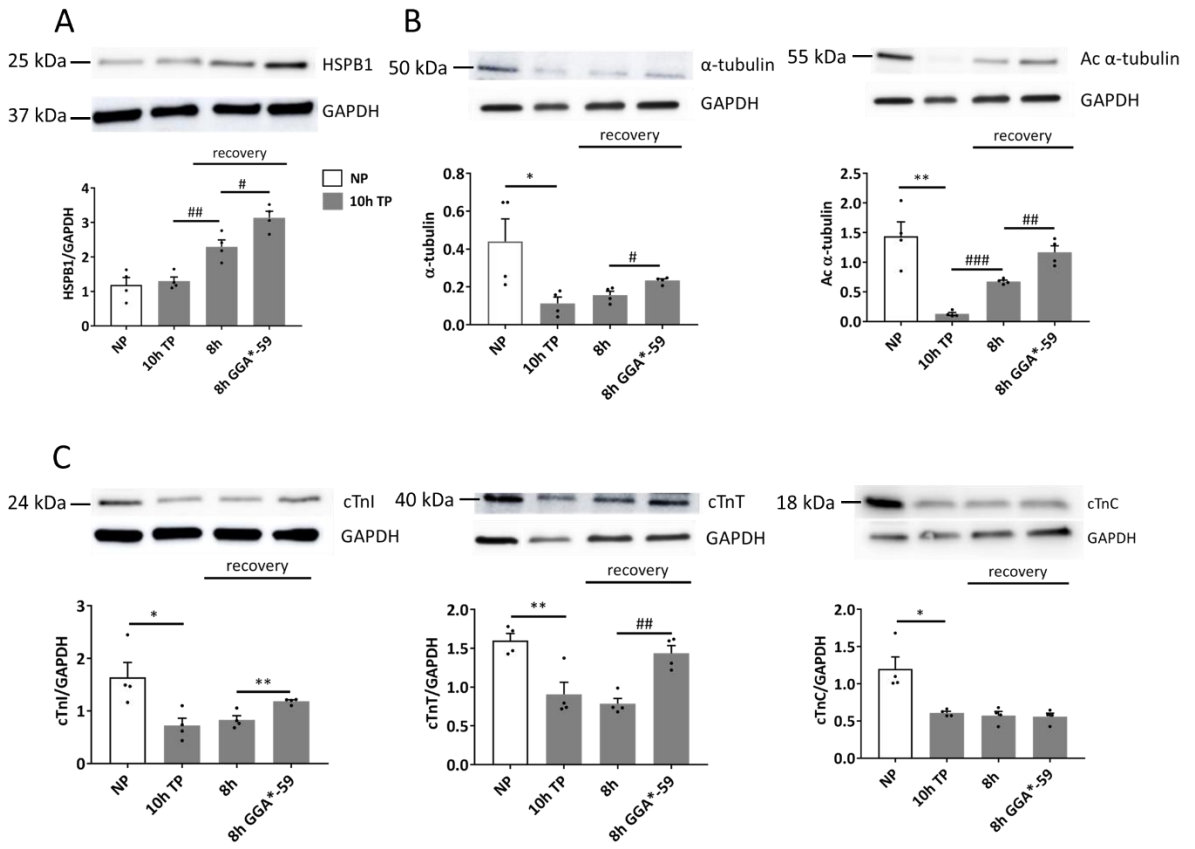

Figure 2. GGA*-59 post-treatment increases HSPB1, restores (acetylated) α-tubulin and cardiac troponin I and troponin T protein levels

(**A**) Representative Western blot and quantified data showing HSPB1 protein levels of HL-1 cardiomyocytes in control non-paced (NP), 10 h tachypaced (TP), and TP with 8 h recovery with DMSO or 10 µM GGA*-59 post-treatment. (**B**) Representative Western blot and quantified data showing reduced α-tubulin and acetylated (Ac) α-tubulin levels after TP and during 8 h recovery with DMSO-treatment, and increased protein expression levels of α-tubulin and acetylated (Ac) α-tubulin by post-treatment of GGA*-59. (**C**) Representative Western blot and quantified data showing that protein expression levels of cTnI, cTnT and cTnC are significantly reduced after 10 h TP and 8 h recovery with DMSO-treatment, and significantly restored by post-treatment with GGA*-59. **P*<0.05 and ***P*<0.01 vs NP, $^{\#}$*P*<0.05, $^{\#\#}$*P*<0.01 and $^{\#\#\#}$*P*<0.001 vs 10 h TP or 8 h recovery. Number of independent experiments N=4.

GGA*-59 post-treatment increases HSPB1 expression and restores (acetylated) α-tubulin, cardiac troponin I and troponin T protein levels

Since we previously showed in tachypaced HL-1 cardiomyocytes that the protective effect of GGA and GGA-derivatives against remodeling is via HSPB1 induction [26], the role of HSPB1 in reversibility from

remodeling is examined. Tachypacing did not alter the expression level of HSPB1, compared to control HL-1 cardiomyocytes. Whereas, HSPB1 levels were significantly increased in tachypaced HL-1 cardiomyocytes after 8 h recovery, and even further enhanced by GGA*-59 post-treatment (Figure 2A). In addition, tachypacing resulted in a significant decrease in α-tubulin and acetylated α-tubulin levels and only acetylated α-tubulin levels were significantly increased after 8 h recovery. GGA*-59 post-treatment for 8 h further enhanced both α-tubulin and acetylated α-tubulin levels compared to tachypaced DMSO-treated HL-1 cardiomyocytes (Figure 2B). Also, tachypacing resulted in significant reductions in cTnI, cTnT and cTnC levels, which maintained reduced after 8 h recovery. Again, GGA*-59 post-treatment significantly improved cTnI and cTnT levels, whereas no effect on cTnC level was observed compared to tachypaced DMSO-treated HL-1 cardiomyocytes (Figure 2C). Taken together, GGA*-59 enhances recovery of contractile and structural protein levels after tachypacing.

GGA*-59 post-treatment increases mRNA levels of α-tubulin, but not cTnI, cTnT and cTnC

As we observed that the protein levels of α-tubulin, cTnI and cTnT were restored by GGA*-59 post-treatment, we next investigated whether GGA*-59 is able to normalize the transcription levels of these structural proteins. Hereto, the mRNA levels of α-tubulin encoding genes, *tuba1a*, *tuba1b*, *tuba1c*, *tuba4a* and *tuba8*, were measured. Tachypacing for 10 h significantly decreased mRNA levels of all measured tubulin genes (Figure 3A). *Tuba1a*, *tuba1b* and *tuba8* mRNA levels remained decreased during 8 h recovery, whereas, *tuba1c* and *tuba4a* mRNA levels significantly increased during recovery (Figure 3A). Post-treatment with GGA*-59 significantly increased mRNA levels of all the measured α-tubulin encoding genes (Figure 3A), implying that GGA*-59 enhances expression of α-tubulin at transcriptional level, thereby contributing to recovery of α-tubulin protein expression. Also, the amount of mRNA of cardiac troponin complexes, *cTnnI3*, *cTnnT2* and *cTnnC1* was examined by RT-qPCR. Surprisingly, mRNA levels of all cardiac troponins were neither altered by tachypacing nor during

recovery after tachypacing (Figure 3B), indicating that the reduction in protein levels of cardiac troponins is not due to repression at the mRNA level.

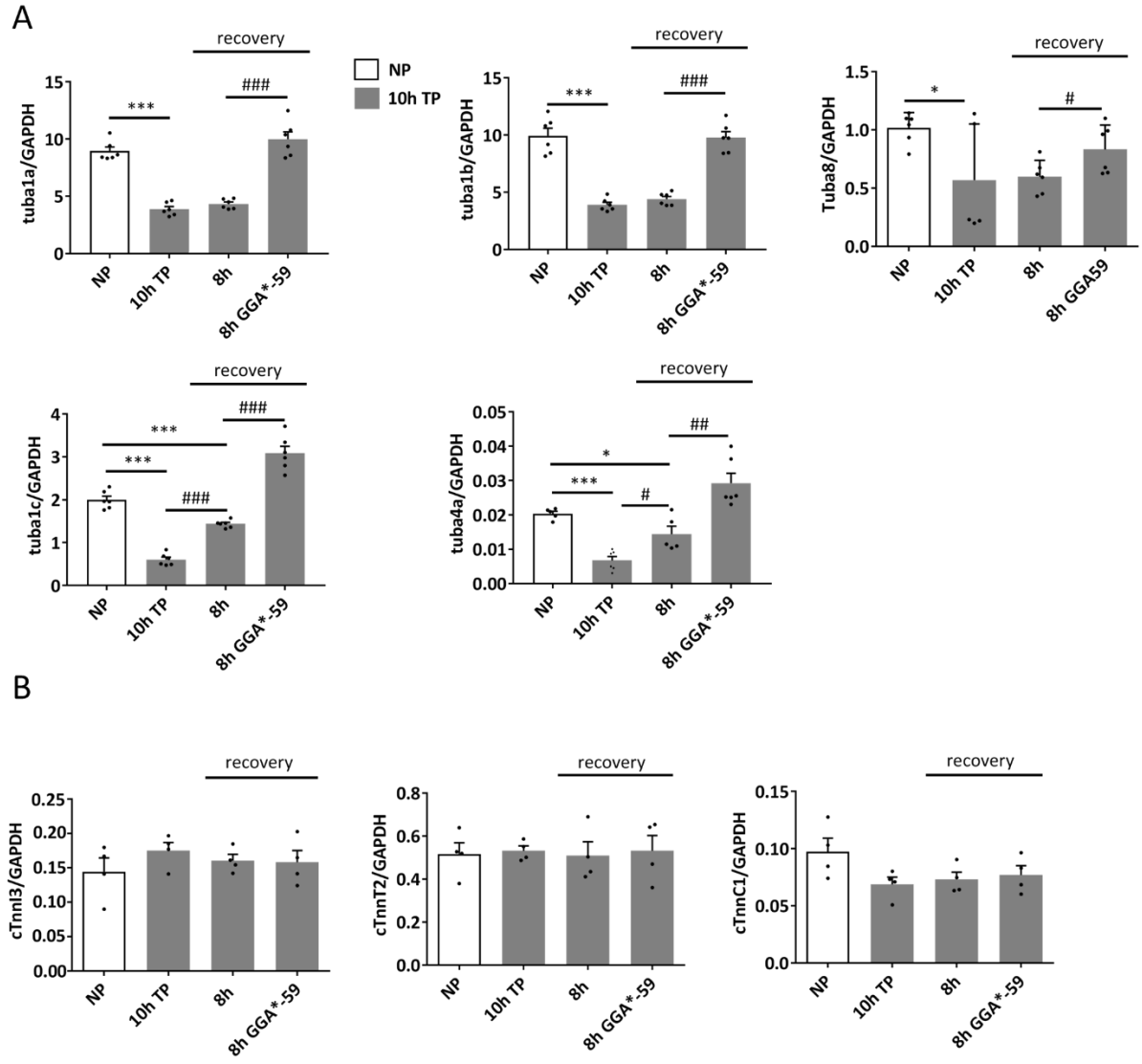

Figure 3. GGA*-59 post-treatment normalizes mRNA levels of α-tubulin encoding genes

(**A**) Quantified RT-qPCR data showing transcription levels of five α-tubulin encoding genes for the conditions as indicated. The mRNA levels are significantly reduced after 10 h TP and TP with 8 h recovery with DMSO-treatment. 8 h post-treatment with GGA*-59 significantly enhances recovery of mRNA levels of all measured α-tubulin genes. The α-tubulin mRNA levels are normalized to the amount of GAPDH. **P*<0.05 and ****P*<0.001 vs NP, $^{\#}P$<0.05, $^{\#\#}P$<0.01 and $^{\#\#\#}P$<0.001 vs 10 h TP or 8 h recovery. Number of independent experiments N=6. (**B**) RT-qPCR data showing that mRNA levels of cTnI, cTnT and cTnC are not altered for the conditions as indicated. Cardiac troponin levels are normalized to the amount of GAPDH. Number of independent experiments N=4.

GGA*-59 post-treatment restores α-tubulin network

Together, the polymerized form of α-tubulin and β-tubulin assembles the microtubule network, which supports the architecture, contractile function and transportation of cytoplasmic constitutes within the cardiomyocyte [31-33]. Previously, we showed that tachypacing induces disruption of the microtubule network via activation of HDAC6, resulting in deacetylation, depolymerization and finally degradation of the depolymerized α-tubulin by calpain. A disrupted microtubule network causes CaT loss and underlies AF progression [12]. To study the role of the microtubule network during recovery after tachypacing, HL-1 cardiomyocytes were subjected to tachypacing, followed by recovery with or without GGA*-59 post-treatment. By using immunofluorescent staining of α-tubulin and acetylated α-tubulin, we observed that the microtubule network gets disrupted due to tachypacing, and partially restores after 8 h recovery (Figure 4A). Interestingly, GGA*-59 post-treatment accelerated recovery of the microtubule network (Figure 4A). Accordingly, the quantified data of the α-tubulin and acetylated α-tubulin-stained microtubule length in each group shows the same trend as the immunofluorescent images exhibit (Figure 4B). Moreover, the immunofluorescent staining indicates that tachypacing-induced disruption of microtubule network was maintained during 24 h recovery, and the post-treatment of GGA*-59 also restored the microtubule network (Figure S4). In addition, we quantified the degree of microtubule disruption, the amount of depolymerized and polymerized α-tubulin was assessed by Western blot analysis. Tachypacing resulted in a significant reduction in both depolymerized and polymerized α-tubulin fractions (Figure 5A, C). Similar to the findings of immunofluorescent staining, GGA*-59 post-treatment enhanced recovery from the tachypacing-induced reduction in depolymerized α-tubulin and acetylated α-tubulin levels (Figure 5A). Whereas, no effect of GGA*-59 on polymerized fractions was observed (Figure 5C). Taken together, the findings suggest that GGA*-59-induced normalization of depolymerized acetylated α-tubulin levels after tachypacing contributes to elongation of the microtubule network [34, 35], which underlies restoration of cardiomyocyte structure and contractile function.

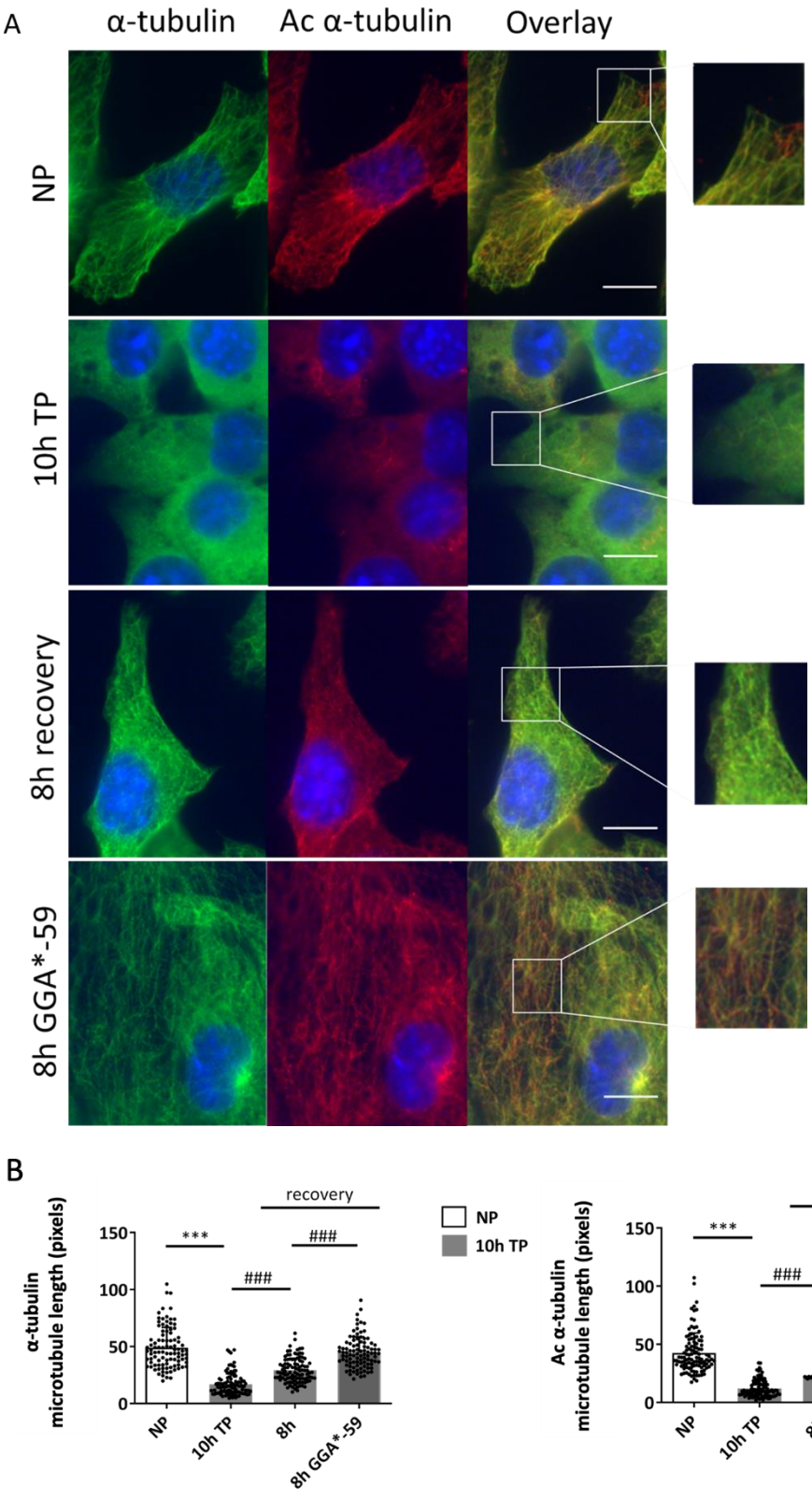

Figure 4. GGA*-59 post-treatment enhances restoration of the microtubule network after tachypacing of HL-1 cardiomyocytes

(**A**) Representative immunofluorescent images showing the microtubule network in HL-1 cardiomyocytes upon control non-paced (NP), 10 h tachypacing (TP), TP with 8 h recovery with DMSO or GGA*-59 post-treatment. TP results in disruption of the microtubule network which remains disrupted after 8 h recovery, GGA*-59 post-treatment accelerates restoration of the microtubule network. The microtubule network is represented by staining of α-tubulin and acetylated (Ac) α-tubulin. Scale bars represent 10 µm, zoomed images are magnified 3x based on the original image. (**B**) Quantified data of the immune-fluorescent images showing that 10 h tachypacing (TP) decreases the length of α-tubulin and acetylated (Ac) α-tubulin-stained microtubules. Upon recovery, the microtubule length increases, but post-treatment with GGA*-59 significantly accelerates the elongation of the microtubules. For each experimental condition, 100 α-tubulin and acetylated (Ac) α-tubulin stained microtubules from 5 to 9 images are selected and quantified by ImageJ. ***P<0.001 vs NP and $^{###}P$<0.001 vs 8h recovery.

GGA*-59 post-treatment induces HSPB1 level in the depolymerized fraction of α-tubulin

As we observed that GGA*-59 post-treatment accelerates restoration of depolymerized acetylated α-tubulin levels after tachypacing, we examined the role of HSPB1 in restoration. The amount of HSPB1 was significantly increased in depolymerized α-tubulin fractions after 8 h post-treatment with GGA*-59 compared to DMSO-treated recovery group (Figure 5B). However, in the polymerized α-tubulin fraction, the HSPB1 level was significantly increased after 10 h TP and maintained increased during 8 h recovery. Importantly, GGA*-59 post-treatment did not further increase the HSPB1 level in the polymerized α-tubulin fractions (Figure 5D). These results indicate that the GGA*-59-induced HSPB1 levels mainly presents in the depolymerized acetylated α-tubulin fractions, and thereby may protect the microtubule network from calpain-induced degradation as previously observed [12]. Binding of HSPB1 to the depolymerized (acetylated) α-tubulin fractions, may represent one of the underlying mechanisms how GGA*-59 improves the conservation of the microtubule network and enhances recovery from tachypacing-induced structural remodeling in HL-1 cardiomyocytes.

Recombinant HSPB1 enhances recovery from contractile dysfunction and microtubule disruption

So far, we showed that pharmacological post-treatment with the HSP-inducer GGA*-59 enhances recovery from tachypacing-induced contractile dysfunction and normalizes contractile and structural protein levels. As we previously showed that GGA and GGA-derivatives protect against the contractile dysfunction in tachypaced atrial cardiomyocytes via HSPB1 [26, 28], we next studied whether recombinant HSPB1 (rcHSPB1) sorts comparable protective effects. Hereto, we transfected HL-1 cardiomyocytes with rcHSPB1 after tachypacing. Interestingly, rcHSPB1 post-treatment enhanced recovery from tachypacing-induced CaT loss in HL-1 cardiomyocytes, compared to tachypaced chariot reagent-treated cardiomyocytes (Figure 6A, B).

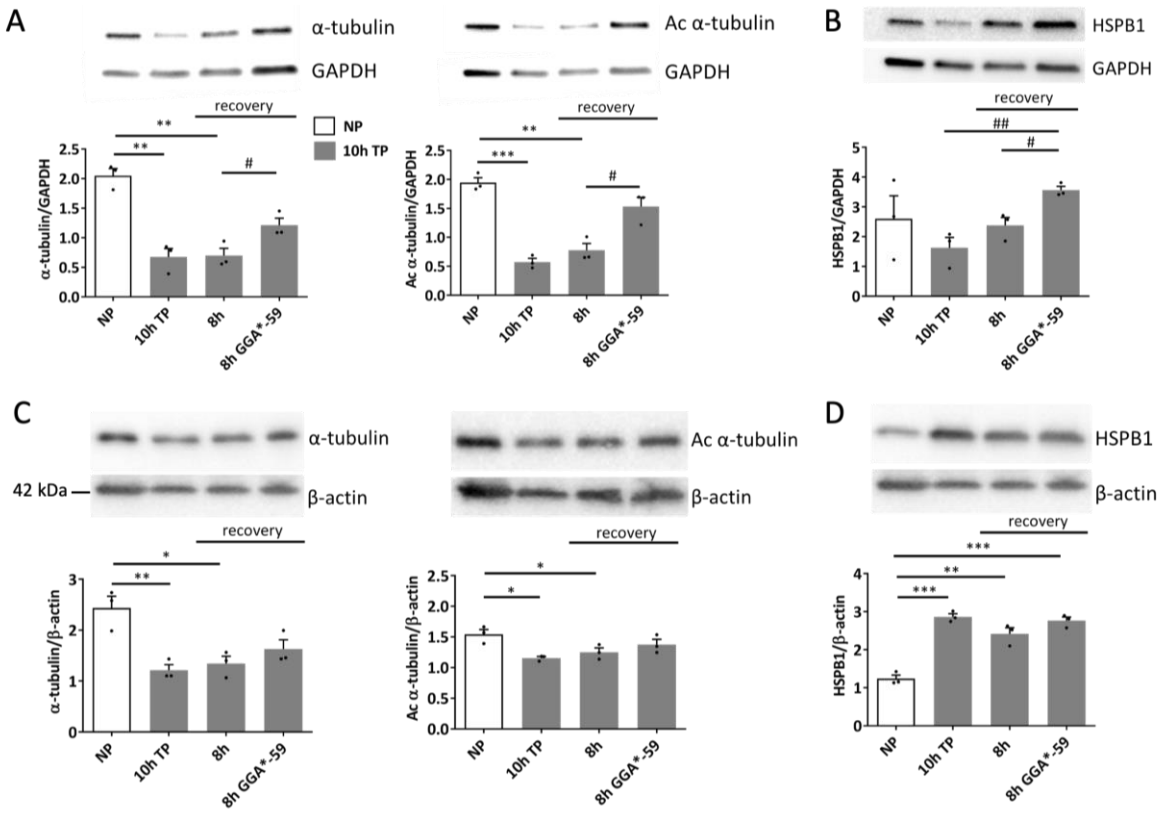

Figure 5. GGA*-59 post-treatment restores the depolymerized fractions of α-tubulin and acetylated α-tubulin, which is associated with increased HSPB1 levels in the depolymerized α-tubulin fractions

(**A**) Representative Western blot images and quantified data showing that α-tubulin and acetylated (Ac) α-tubulin levels are decreased in the depolymerized fractions of α-tubulin after 10 h TP and 8 h recovery with DMSO post-treatment. Both levels are significantly recovered by 8 h post-treatment with GGA*-59. (**B**) Representative Western blot images and quantified data showing that the HSPB1 amount is increased in the depolymerized α-tubulin fractions of α-tubulin after 8 h post-treatment with GGA*-59. (**C**) Representative Western blot images and quantified data showing that α-tubulin and Ac α-tubulin levels are decreased in the polymerized fractions after 10 h TP and 8 h recovery with DMSO-treatment, and not recovered by post-treatment with GGA*-59. (**D**) Representative Western blot images and quantified data for HSPB1 amount. HSPB1 is enhanced in all conditions after 10 h TP, and no effect of GGA*-59 post-treatment is observed in the polymerized α-tubulin fractions. **P*<0.05, ***P*<0.01 and ****P*<0.001 vs NP and $^{\#}$*P*<0.05 vs 8 h recovery. Number of independent experiments N=3.

In addition, rcHSPB1 significantly restored protein expression levels of (acetylated) α-tubulin (Figure 7A, B, Figure S6), but no effect on cTnI, cTnT and cTnC was observed (Figure 7C, Figure S6). Next, we examined whether HSPB1 can affect the transcription level of α-tubulin during recovery after tachypacing of HL-1 cardiomyocytes. As expected, the tachypacing-induced reduction in mRNA level

of the α-tubulin encoding gene *tuba1a* maintained reduced after recovery with chariot reagent incubation, but was significantly enhanced by rcHSPB1 post-treatment (Figure S5). Taken together, these findings show that HSPB1 enhances restoration of α-tubulin and acetylated α-tubulin, but not cardiac troponins levels after tachypacing.

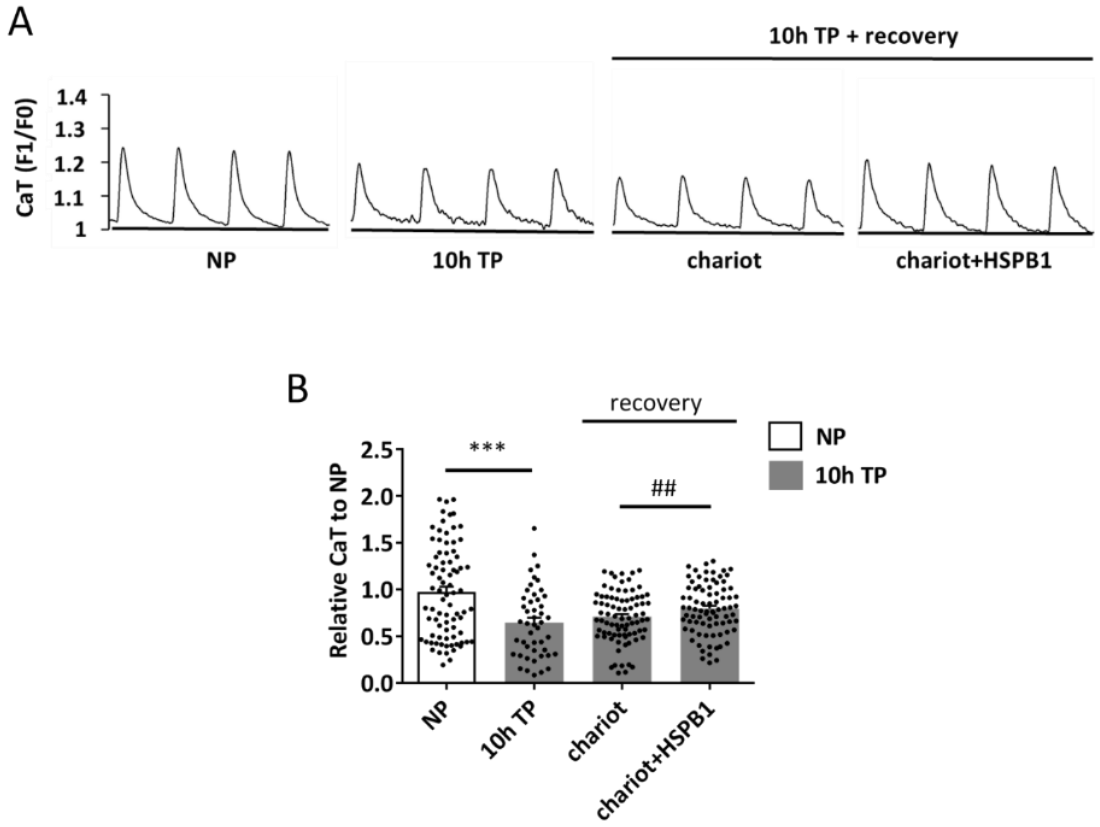

Figure 6. HSPB1 recovers contractile function in HL-1 cardiomyocytes after tachypacing

(**A**) Representative CaT and (**B**) quantified CaT amplitudes of control non-paced (NP), 10 h tachypaced (TP), TP with 3 h control chariot or TP with 3 h chariot rcHSPB1 post-treatment in HL-1 cardiomyocytes. TP induces significant CaT loss, which remains reduced during 3 h recovery with chariot reagent. In contrast, 3 h transfection of chariot rcHSPB1 significantly enhances recovery from CaT loss in HL-1 cardiomyocytes. ***P<0.001 vs NP and $^{\#\#}P$<0.001 vs chariot. N (NP)=81, N (10h TP)=47, N (chariot)=82, N (chariot+HSPB1)=82.

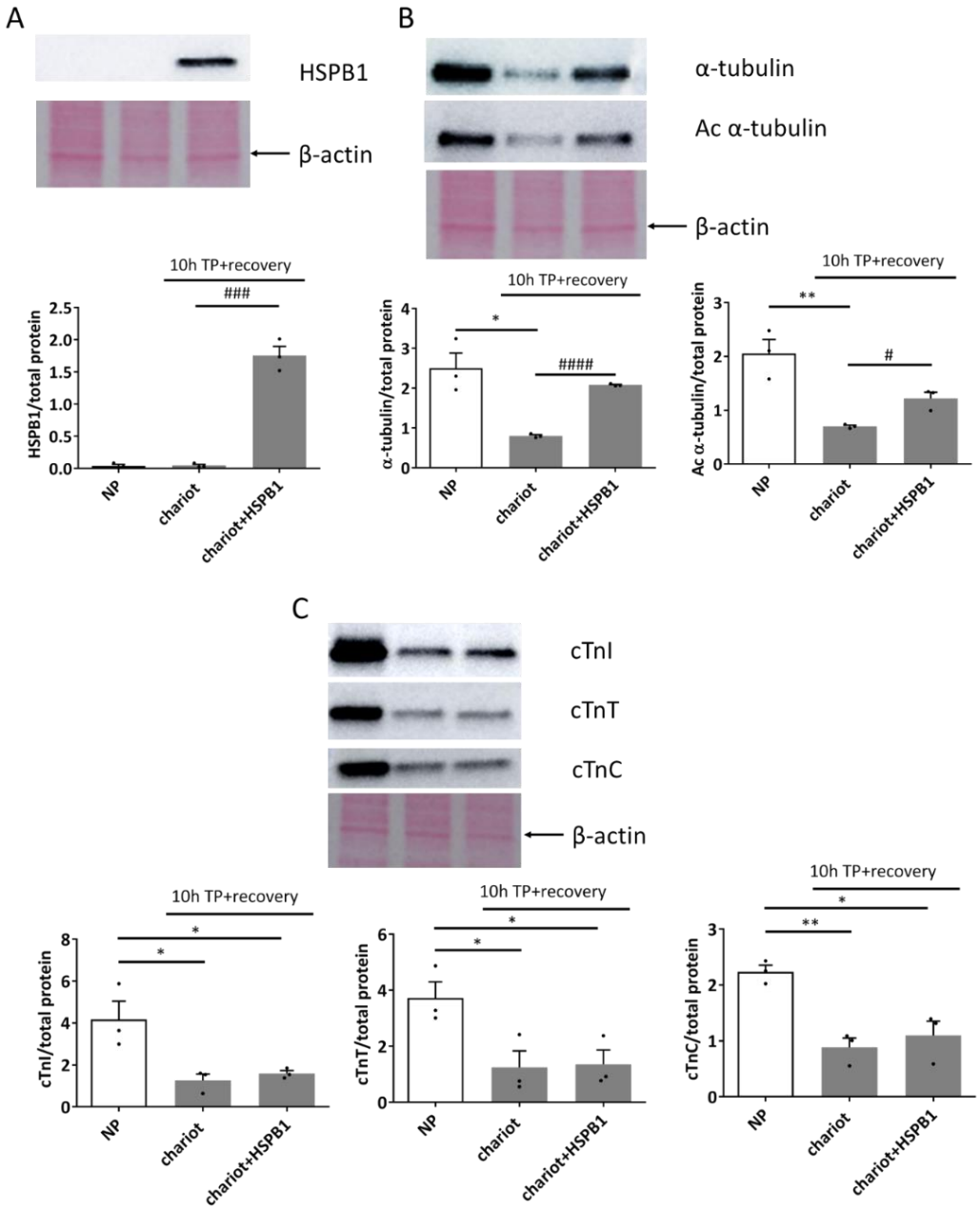

Figure 7. HSPB1 normalizes α-tubulin and acetylated α-tubulin and not cardiac troponin levels in tachypaced HL-1 cardiomyocytes

(**A**) Representative Western blot images and quantified data showing recombinant HSPB1 (rcHSPB1) is successfully transfected in the HL-1 cardiomyocytes. (**B**) Representative Western blot images and quantified data showing 10 h tachypacing (TP) results in reductions in α-tubulin and Ac α-tubulin levels, which maintain reduced during 3 h recovery with chariot reagent, but are significantly recovered by transfection with rcHSPB1. (**C**) Representative Western blot images and quantified data showing 10 h TP results in reductions in protein expression levels of cTnI, cTnT and cTnC, which maintain during both 3 h recovery with chariot reagent and transfection of rcHSPB1. **P*<0.5 and ***P*<0.01 vs NP, $^{\#}$*P*<0.05, $^{\#\#\#}$*P*<0.001 and $^{\#\#\#\#}$*P*<0.0001 vs chariot. Number of independent experiments N=3.

GGA*-59 and rcHSPB1 post-treatment repress HDAC6 activity in tachypaced HL-1 cardiomyocytes

In our previous study we demonstrated that tachypacing-induced HDAC6 activation results in deacetylation, depolymerization and finally degradation of the depolymerized α-tubulin by calpain [12]. To examine whether GGA*-59 and rcHSPB1 post-treatment enhance the recovery of (acetylated) α-tubulin levels via attenuation of HDAC6 and/or calpain activity, HL-1 cardiomyocytes were tachypaced, followed by 8 h recovery with and without GGA*-59 or rcHSPB1 post-treatment.

As expected, 10 h TP increased HDAC6 activity and both GGA*-59 and rcHSPB1 post-treatment significantly reduced HDAC6 activity (Figure 8A, B). Furthermore, tachypacing increased calpain activity levels, which maintained increased during 8 h recovery. GGA*-59 post-treatment did not normalize the tachypacing-induced increase in calpain activity (Figure 8C), indicating that the enhanced recovery of α-tubulin, acetylated α-tubulin, cTnI and cTnT levels by GGA*-59 is not via repression of calpain activity. As reduced HDAC6 activity results in increased acetylated α-tubulin levels, which are protected from calpain-induced degradation [12], the current findings suggest that restoration of (acetylated) α-tubulin by GGA*-59 and rcHSPB1, may result from reduction in HDAC6 activity. Whether the attenuation of HDAC6 activity underlies the restoration of cTnI and cTnT is unknown.

Discussion

This study shows that post-treatment with the HSP-inducing compound GGA*-59 increases HSPB1 expression and enhances recovery from tachypacing-induced contractile dysfunction in HL-1 cardiomyocytes. At the molecular level, GGA*-59 post-treatment restores the microtubule network and both transcriptional and protein levels of (acetylated) α-tubulin. Furthermore, GGA*-59 enhances recovery of depolymerized (acetylated) α-tubulin fractions, which coincides with elevated HSPB1 binding, suggesting a role for HSPB1 in stabilizing the microtubule network. Moreover, GGA*-59 restores the sarcomere proteins cTnI and cTnT levels, without affecting the mRNA expression of

troponin encoding genes. Comparable protective effects were observed by HSPB1 overexpression. Recombinant HSPB1 also restores tachypacing-induced CaT loss, (acetylated) α-tubulin protein and mRNA levels, yet does not recover cardiac troponins. Intriguingly, the tachypacing-induced activity of HDAC6, whose major cytosolic substrate is acetylated α-tubulin, is suppressed by both GGA*-59 and recombinant HSPB1, suggesting that part of the beneficial effects on cardiomyocyte recovery are via attenuation of HDAC6 activity.

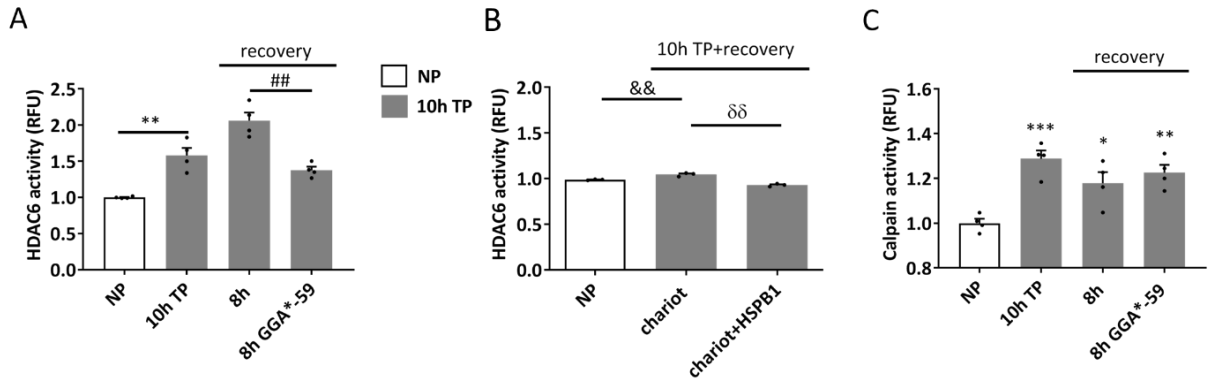

Figure 8. GGA*-59 post-treatment and rcHSPB1 transfection suppress HDAC6 and not calpain activity in tachypaced HL-1 cardiomyocytes

(**A**) 10 h tachypacing (TP) induces HDAC6 activity, which remains increased during 8 h recovery with DMSO post-treatment. HDAC6 activity is suppressed by 8 h post-treatment with GGA*-59 in HL-1 cardiomyocytes. $^{**}P<0.01$ vs NP and $^{\#\#}P<0.01$ vs 8h recovery. Number of independent experiments N=4. (**B**) 10 h TP induces HDAC6 activity which maintains increased during 3 h recovery of HL-1 cardiomyocytes treated with chariot reagent. In contrast, HDAC6 activity is significantly suppressed by rcHSPB1 transfection in TP HL-1 cardiomyocytes. $^{\&\&}P<0.01$ vs NP and $^{\delta\delta}P<0.01$ vs chariot. Number of independent experiments N=2. (**C**) 10 h TP increases calpain activity, which maintains increased during 8 h recovery with DMSO or GGA*-59 post-treatment in HL-1 cardiomyocytes. $^{*}P<0.05$, $^{**}P<0.01$ and $^{***}P<0.001$ vs NP. Number of independent experiments N=4.

Accelerated cardiomyocyte recovery via restoration of microtubule network

The findings from this study point to restoration of the microtubule network as a key feature in the recovery from structural and functional remodeling upon tachypacing. The observation is

strengthened by our observation that GGA*-59 and recombinant HSPB1 accelerate recovery of mRNA and protein levels of (acetylated) α-tubulin. In addition, GGA*-59 accelerates recovery of depolymerized (acetylated) α-tubulin fractions and elevates HSPB1 levels in these fractions. Finally, GGA*-59 and recombinant HSPB1 suppress HDAC6 activity, thereby preventing deacetylation, depolymerization and finally degradation of α-tubulin by calpain as shown before [12]. Although a significant induction in HDAC6 activity was observed in tachypaced HL-1 cardiomyocytes treated with chariot reagent, the induction was minor. As the chariot peptide is designed to form non-covalent complexes with other proteins [36], the chariot peptide may interact with HDAC6 and thereby reduce its activation.

It is known that the microtubule network is a dynamic structure, in which the depolymerized and polymerized forms of α-tubulin occur in a balanced status [37]. Especially, acetylated α-tubulin is a hallmark for microtubule stability and integrity [38, 39]. Our previous study showed that patients with paroxysmal and persistent AF reveal reductions in (acetylated) α-tubulin levels in atrial tissue, which coincides with increased HDAC6 expression and activity. Also, tachypacing induced disruption of the microtubule network via deacetylation, depolymerization and finally degradation of depolymerized α-tubulin by calpain, in HL-1 cardiomyocytes, *Drosophila* and a dog model for AF. In line, conservation of the microtubule network by an HDAC6 inhibitor, prevented AF progression in these experimental model systems [12]. The findings indicate that microtubule-related structural remodeling represents a key modulator that obstructs the recovery of cardiomyocytes from contractile dysfunction in AF. Indeed, in the current study, we found that tachypacing disrupts the microtubule network resulting in CaT loss, which both maintain impaired during recovery. GGA*-59 and recombinant HSPB1 post-treatment restored the microtubule network and CaT loss. Interestingly, GGA*-59 also restored acetylated α-tubulin expression and enhanced HSPB1 levels especially in the depolymerized fractions, whereas, α-tubulin expression in the polymerized fractions was not restored. Studies have shown that the depolymerized tubulin fractions consist of tubulin dimers and oligomers [40-42]. Also, tubulin dimers are less preferable than the polymers to become acetylated [38]. These studies suggest that

the acetylated α-tubulin observed in the depolymerized fractions may represent a mixture of acetylated tubulin dimers and oligomers. HSPB1 is known to bind to contractile and structural proteins to conserve their function and shield them from degradation by proteases, such as calpain [43-45]. This may also occur in tachypaced HL-1 cardiomyocytes, as an induction in calpain activity was observed, which maintained increased during recovery and GGA*-59 post-treatment. Despite this maintained increase in calpain activity, α-tubulin levels were significantly recovered in GGA*-59 post-treated cardiomyocytes, suggesting that HSPB1 may protect against calpain-induced degradation of deacetylated and depolymerized α-tubulin. Findings from the literature affirm this role of HSPB1. First, it has been shown that HSPB5 prevents aggregation of tubulin via its α-crystallin core domain, and thereby conserves the microtubule integrity under stressful conditions [46-48]. The amino acid sequence exposed at the surface of α-crystallin core domain recognizes and interacts with a homologous sequence identified on the tubulin surface [49, 50]. Also HSPB1 shares the α-crystallin core domain in its structure [51] and was found to associate with both α-tubulin/β-tubulin dimers in Hela cells [52], and protect the stability of microtubules under the acidic environment presents in a tumor model of Chinese hamster ovary (CHO) cells [53]. Second, the elevated depolymerized α-tubulin levels, present after GGA*-59 post-treatment, may be incorporated into the damaged microtubules to aid to the recovery of the network. This act of self-repair has been described in *in vitro* experiments for stress-induced disruption of the microtubule network. Here, the disrupted network incorporates free circulating α-tubulin dimers into the pre-existing α-tubulin network, thereby fixing the impaired sites and initiating elongation and conservation of the microtubule network [34, 35, 54]. In line, we also observed the recovery of microtubule network via immunofluorescent microscopy. GGA*-59 post-treatment of tachypaced HL-1 cardiomyocytes showed intact microtubules of (acetylated) α-tubulin with increased length, in contrast to the microtubules with short length observed in non-treated HL-1 cardiomyocytes. The observed microtubules with increased length after GGA*-59 post-treatment may be a result of the self-repair mechanisms. Finally, GGA*-59 and rcHSPB1 post-treatment normalized tachypacing-induced HDAC6 activity in HL-1 cardiomyocytes during recovery after tachypacing. In our

previous study, we demonstrated the crucial role of HDAC6 activity in AF progression by disruption of the microtubule network [12]. The suppressed HDAC6 activity may decrease the amount of deacetylated α-tubulin, thereby protecting α-tubulin from being depolymerized and degraded by calpain during tachypacing. As such, GGA*-59 and rcHSPB1 may also contribute by restoring the stability of the microtubule network via suppression of HDAC6 activity. One possibility of how GGA*-59 may suppress HDAC6 activity is via HSPB1. It was shown that HDAC6 is one of the client proteins of HSPB1, they directly interact with each other [55]. Binding of HDAC6 to HSPB1 may suppress its activity. Further research should elucidate the effect of HSPB1 on HDAC6 activity and modulation of the microtubule network in AF.

GGA*-59 and rcHSPB1 normalize mRNA levels of tubulin genes

Next to restoration of the microtubule network via prevention of tachypacing-induced degradation, GGA*-59 also restored mRNA levels of all the tubulin genes measured. The restored α-tubulin encoding genes may contribute to the recovery of protein expression levels of α-tubulin and thereby enhance the pool of α-tubulin in the cytosol that can be used for acetylation and restoration of the microtubule network. Since rcHSPB1 also increased tubulin gene expression, HSPB1 may have a direct effect on transcription of tubulin genes. One previous study revealed that nuclear HSPB1 can directly activate transcription factor SP1 and thereby regulate gene expression, resulting in neuronal protection [56]. Whether HSPB1 activates transcription factors resulting in tubulin expression is unknown. Further research should elucidate whether the promoter regions and/or transcription factors can be directly regulated via HSPB1. Also the cause of TP-induced reduction in mRNA expression level of all the α-tubulin genes measured is not known. Previous studies revealed that depolymerized α-tubulin binds to α-tubulin mRNA associated to ribosomes, resulting in its degradation and destabilization [57-59]. Whether this autoregulatory mechanism of tubulin expression is also activated upon tachypacing is unknown.

Conclusions

Our findings indicate that the HSP inducer GGA*-59 and recombinant HSPB1 enhance recovery from tachypacing-induced structural remodeling and contractile dysfunction in HL-1 cardiomyocytes. GGA*-59 increases HSPB1 expression, represses HDAC6 activity and restores contractile protein and microtubule expression after tachypacing. The results imply that HSPB1 represents a druggable target to enhance recovery from AF-induced remodeling.

Acknowledgements

This work was supported by the Dutch Heart Foundation (2013T096, 2013T144, 2017T029); the Netherlands Cardiovascular Research Initiative and Dutch Heart Foundation CVON2014-40 DOSIS and CVON-STW2016-14728 AFFIP and LSH-TKI (40-43100-98-008). We are grateful to C.A.M. Jongenelen from the Anatomy and neurosciences department of VUmc for helping with the fluorometric reader, F. Hoogstra-Berends UMCG for technical assistance, A. Heeres from Syncom BV for synthesizing GGA*-59 and H. Steen Chaperone Pharma for providing GGA*-59.

Conflict of interest

None declared.

References

1. Krijthe BP, et al. Projections on the number of individuals with atrial fibrillation in the European Union, from 2000 to 2060. Eur Heart J. 2013;34:2746-51.
2. Morillo CA, et al. Atrial fibrillation: the current epidemic. J Geriatr Cardiol. 2017;14:195-203.
3. Magnani JW, et al. Atrial fibrillation: current knowledge and future directions in epidemiology and genomics. Circulation. 2011;124:1982-93.

4. Weil BR and Ozcan C. Cardiomyocyte Remodeling in Atrial Fibrillation and Hibernating Myocardium: Shared Pathophysiologic Traits Identify Novel Treatment Strategies? Biomed Res Int. 2015;2015:587361.
5. Zakeri R, et al. The burden of proof: The current state of atrial fibrillation prevention and treatment trials. Heart Rhythm. 2017;14:763-82.
6. Aronow WS. Management of the older person with atrial fibrillation. The journals of gerontology Series A, Biological sciences and medical sciences. 2002;57:M352-63.
7. Dobrev D, et al. Novel molecular targets for atrial fibrillation therapy. Nat Rev Drug Discov. 2012;11:275-91.
8. Therkelsen SK, et al. Atrial and ventricular volume and function evaluated by magnetic resonance imaging in patients with persistent atrial fibrillation before and after cardioversion. Am J Cardiol. 2006;97:1213-9.
9. Ng KK and Skanes AC. When it comes to atrial fibrillation recurrence, perhaps we should look both left and right. Can J Cardiol. 2015;31:17-9.
10. Ke L, et al. Calpain mediates cardiac troponin degradation and contractile dysfunction in atrial fibrillation. Journal of molecular and cellular cardiology. 2008;45:685-93.
11. Brundel BJ, et al. Heat shock protein upregulation protects against pacing-induced myolysis in HL-1 atrial myocytes and in human atrial fibrillation. Journal of molecular and cellular cardiology. 2006;41:555-62.
12. Zhang D, et al. Activation of histone deacetylase-6 induces contractile dysfunction through derailment of alpha-tubulin proteostasis in experimental and human atrial fibrillation. Circulation. 2014;129:346-58.
13. Ausma J, et al. Structural changes of atrial myocardium due to sustained atrial fibrillation in the goat. Circulation. 1997;96:3157-63.
14. Brundel BJ, et al. Molecular mechanisms of remodeling in human atrial fibrillation. Cardiovascular research. 2002;54:315-24.
15. Allessie M. The "second factor": a first step toward diagnosing the substrate of atrial fibrillation? Journal of the American College of Cardiology. 2009;53:1192-3.
16. Zhang D, et al. Effects of different small HSPB members on contractile dysfunction and structural changes in a Drosophila melanogaster model for Atrial Fibrillation. Journal of molecular and cellular cardiology. 2011;51:381-9.
17. Ke L, et al. HSPB1, HSPB6, HSPB7 and HSPB8 protect against RhoA GTPase-induced remodeling in tachypaced atrial myocytes. PloS one. 2011;6:e20395.
18. Penke B, et al. Heat Shock Proteins and Autophagy Pathways in Neuroprotection: from Molecular Bases to Pharmacological Interventions. Int J Mol Sci. 2018;19.
19. Smith HL, et al. Molecular chaperones and neuronal proteostasis. Semin Cell Dev Biol. 2015;40:142-52.
20. Henning RH and Brundel B. Proteostasis in cardiac health and disease. Nat Rev Cardiol. 2017;14:637-53.
21. Jee H. Size dependent classification of heat shock proteins: a mini-review. J Exerc Rehabil. 2016;12:255-9.
22. Hu X, et al. The protective role of small heat shock proteins in cardiac diseases: key role in atrial fibrillation. Cell stress & chaperones. 2017;22:665-74.
23. Mercer EJ, et al. Hspb7 is a cardio-protective chaperone facilitating sarcomeric proteostasis. Dev Biol. 2018;435:41-55.
24. Tucker NR and Shelden EA. Hsp27 associates with the titin filament system in heat-shocked zebrafish cardiomyocytes. Exp Cell Res. 2009;315:3176-86.
25. Sakamoto K, et al. Translocation of HSP27 to sarcomere induced by ischemic preconditioning in isolated rat hearts. Biochem Biophys Res Commun. 2000;269:137-42.
26. Brundel BJ, et al. Induction of heat shock response protects the heart against atrial fibrillation. Circ Res. 2006;99:1394-402.

27. Hoogstra-Berends F, et al. Heat shock protein-inducing compounds as therapeutics to restore proteostasis in atrial fibrillation. Trends Cardiovasc Med. 2012;22:62-8.
28. van Marion DM, et al. Screening of novel HSP-inducing compounds to conserve cardiomyocyte function in experimental atrial fibrillation. Drug Des Devel Ther. 2019;13:345-64.
29. Wiersma M, et al. Endoplasmic Reticulum Stress Is Associated With Autophagy and Cardiomyocyte Remodeling in Experimental and Human Atrial Fibrillation. Journal of the American Heart Association. 2017;6(10):e006458.
30. Zhang D, et al. DNA damage-induced PARP1 activation confers cardiomyocyte dysfunction through NAD+ depletion in experimental Atrial Fibrillation. Nature Communications. 2019; 21;10(1):1307.
31. Kaverina I and Straube A. Regulation of cell migration by dynamic microtubules. Seminars in cell & developmental biology. 2011;22:968-74.
32. Robison P and Prosser BL. Microtubule mechanics in the working myocyte. The Journal of physiology. 2017;595:3931-7.
33. Pritchard HAT, et al. Microtubule structures underlying the sarcoplasmic reticulum support peripheral coupling sites to regulate smooth muscle contractility. Science signaling. 2017;10.
34. Aumeier C, et al. Self-repair promotes microtubule rescue. Nature cell biology. 2016;18:1054-64.
35. Schaedel L, et al. Microtubules self-repair in response to mechanical stress. Nature materials. 2015;14:1156-63.
36. Morris MC, et al. A peptide carrier for the delivery of biologically active proteins into mammalian cells. Nature Biotechnology. 2001; 19 (12): 1173-6.
37. Bowne-Anderson H, et al. Microtubule dynamic instability: a new model with coupled GTP hydrolysis and multistep catastrophe. BioEssays : news and reviews in molecular, cellular and developmental biology. 2013;35:452-61.
38. Maruta H, et al. The acetylation of alpha-tubulin and its relationship to the assembly and disassembly of microtubules. J Cell Biol. 1986;103:571-9.
39. Liu N, et al. New HDAC6-mediated deacetylation sites of tubulin in the mouse brain identified by quantitative mass spectrometry. Sci Rep. 2015;5:16869.
40. Mozziconacci J, al. Tubulin dimers oligomerize before their incorporation into microtubules. PloS one. 2008;3:e3821.
41. Galbraith JA, et al. Slow transport of unpolymerized tubulin and polymerized neurofilament in the squid giant axon. Proceedings of the National Academy of Sciences of the United States of America. 1999;96:11589-94.
42. Liu J and Lessman CA. Soluble tubulin complexes, gamma-tubulin, and their changing distribution in the zebrafish (Danio rerio) ovary, oocyte and embryo. Comparative biochemistry and physiology Part B, Biochemistry & molecular biology. 2007;147:56-73.
43. Martinez-Laorden E, et al. Expression of heat shock protein 27 and troponin T and troponin I after naloxone-precipitated morphine withdrawal. European journal of pharmacology. 2015;766:142-50.
44. Blunt BC, et al. H2O2 activation of HSP25/27 protects desmin from calpain proteolysis in rat ventricular myocytes. American journal of physiology Heart and circulatory physiology. 2007;293:H1518-25.
45. Bryantsev AL, et al. Distribution, phosphorylation, and activities of Hsp25 in heat-stressed H9c2 myoblasts: a functional link to cytoprotection. Cell stress & chaperones. 2002;7:146-55.
46. Ohto-Fujita E, et al. Analysis of the alphaB-crystallin domain responsible for inhibiting tubulin aggregation. Cell stress & chaperones. 2007;12:163-71.

47. Sakurai T, et al. The decrease of the cytoskeleton tubulin follows the decrease of the associating molecular chaperone alphaB-crystallin in unloaded soleus muscle atrophy without strech. FASEB J. 2005;19(9):1199-201.
48. Bluhm WF, et al. Specific heat shock proteins protect microtubules during simulated ischemia in cardiac myocytes. Am J Physiol. 1998;275:H2243-9.
49. Ghosh JG, et al. Interactive domains in the molecular chaperone human alphaB crystallin modulate microtubule assembly and disassembly. PloS one. 2007;2:e498.
50. Houck SA and Clark JI. Dynamic subunit exchange and the regulation of microtubule assembly by the stress response protein human alphaB crystallin. PloS one. 2010;5:e11795.
51. Weeks SD, et al. Characterization of human small heat shock protein HSPB1 alpha-crystallin domain localized mutants associated with hereditary motor neuron diseases. Sci Rep. 2018;8:688.
52. Hino M, et al. Small heat shock protein 27 (HSP27) associates with tubulin/microtubules in HeLa cells. Biochem Biophys Res Commun.2000;271(1):164-9.
53. Hargis MT, et al. Hsp27 anti-sense oligonucleotides sensitize the microtubular cytoskeleton of Chinese hamster ovary cells grown at low pH to 42 degrees C-induced reorganization. Int J Hyperthermia. 2004;20:491-502.
54. Dye RB, et al. End-stabilized microtubules observed in vitro: stability, subunit, interchange, and breakage. Cell motility and the cytoskeleton. 1992;21:171-86.
55. Gibert B, et al. Knock down of heat shock protein 27 (HspB1) induces degradation of several putative client proteins. PloS one. 2012;7:e29719.
56. Friedman MJ, et al. Activation of gene transcription by heat shock protein 27 may contribute to its neuronal protection. The Journal of biological chemistry. 2009;284:27944-51.
57. Gay DA, et al. Autoregulatory control of beta-tubulin mRNA stability is linked to translation elongation. Proceedings of the National Academy of Sciences of the United States of America. 1989;86:5763-7.
58. Ben-Ze'ev A, et al. Mechanisms of regulating tubulin synthesis in cultured mammalian cells. Cell. 1979;17:319-25.
59. Gasic I and Mitchison TJ. Autoregulation and repair in microtubule homeostasis. Current opinion in cell biology. 2019;56:80-7.

Supplementary Materials and Methods

HL-1 atrial cardiomyocyte reversibility model and calcium transient measurements

HL-1 cardiomyocytes, obtained from dr. William Claycomb Lab (Louisiana state university, New Orleans), were derived from adult mouse atria, and cultured in complete Claycomb medium (Sigma), supplemented with 10% FBS (PAA cell culture company), 100 µg/ml penicillin/streptomycin (Lonza BioWhittaker), 0.1 mM norepinephrine (Sigma), 2 mM L-glutamine (Lonza BioWhittaker), in 0.02% gelatin (Sigma) coated cell culture plates [1]. The cardiomyocytes were tachypaced (TP, 5 Hz, 40 V and

20 ms pulse duration) with a C-pace100 culture pacer (IonOptix) for 10 h, followed by 8, 16 or 24 h recovery. For calcium transient (CaT) measurement, HL-1 cardiomyocytes were washed with Dulbecco's Modified Eagle Medium (DMEM, Gibco) for 3 times, followed by incubation with 2 μM calcium indicator Fluo-4-AM dye (Invitrogen) in the DMEM medium for 30 min at 37°C, then wash with the DMEM medium for 3 times and incubated with the full Claycomb medium for CaT measurement. CaT of the cardiomyocytes were measured by using IonOptix CaT set-up. The Fluo-4 loaded HL-1 cardiomyocytes were tachypaced at 1 Hz, 40 V, pulse duration of 20 ms, at 37°C. The amplitude of CaT was calculated to indicate the contractile function of cardiomyocytes. To compare the fluorescent signal between each measurement, the signal was calibrated as ΔCaT=F1/F0, F1 stands for the fluorescent signal at any given time, F0 stands for the fluorescent signal at the rest status, which was also described in the previous studies [2, 3].

Protein isolation and Western blot analysis

HL-1 cardiomyocytes were lysed on ice by the radioimmunoprecipitation assay (RIPA) buffer supplemented with protease inhibitor cocktail (Roche), sodium orthovanadate (Sigma), sodium fluoride (Sigma) and β-mercaptoethanol (BioRad), followed by shearing DNA with an insulin needle and measuring protein concentration with Bradford assay (BioRad). After the sample preparation, the protein homogenates were separated on SDS-PAGE gels, transferred to nitrocellulose membranes, probed with primary antibodies (species and dilution time are listed in Table S1): anti-HSPB1 (HSP25, Enzolifesciences), anti-HSPB1 (HSP27, Enzolifesciences), anti-α-tubulin (Sigma), anti-acetylated α-tubulin (Sigma), anti-cardiac troponin I (cTnI, Abcam), anti-cardiac troponin T (cTnT, Abcam), anti-cardiac C (cTnC, Invitrogen), GAPDH (Fitzgerald) and β-actin (Abcam) overnight at 4°C, followed by incubation with horseradish peroxidase-conjugated anti-mouse or anti-rabbit secondary antibodies (Dako, 1:2000) for 1-2 h at room temperature (RT). The intensity of the bands was quantified by using ImageQuant (GE Healthcare).

Chariot transfection of recombinant HSPB1 in tachypaced HL-1 cardiomyocytes

HL-1 cardiomyocytes were seeded on 0.02% gelatin coated coverslips in a 24-well plate. Experimental groups included control non-paced (NP), 10 h TP+3 h recovery with chariot and 10 h TP+3 h recovery with chariot+HSPB1. To transfect recombinant HSPB1 (rcHSPB1) into the cardiomyocytes, the quick protein transfection procedure was performed by using a chariot protein delivery reagent kit (Activemotif). Hereto, 0.67 µl of rcHSPB1 (1.5 mg/ml) was diluted into 50 µl PBS to result in 1 µg rcHSPB1 in one Eppendorf tube. Next, in another tube, 2 µl chariot reagent was added to 50 µl sterilized H_2O. Both tubes were combined followed by incubation at RT for 30 min. After TP for 10 h, the coverslips were immediately transferred to a 24-well plate, followed by washing of the cardiomyocytes with PBS once, and addition of 100 µl chariot-sterilized H_2O vehicle and 100 µl Claycomb medium (-FBS) to the control recovery group, and 100 µl rcHSPB1-chariot complex with 100 µl Claycomb medium (-FBS) to the HSPB1 transfection group, and incubation for 1 h at 37 °C. Finally, 300 µl full Claycomb medium (+FBS) was added to the mixture of each group at 37 °C and incubated for 2 h.

Calpain activity measurement

HL-1 cardiomyocytes were grown on 0.02% gelatin coated 4-well cell culture plates, followed by 10 h TP. The calpain activity was measured by using calpain activity fluorometric assay kit (BioVision) and the fluorometric reader (FLUOstar, BMG Labtechnologies). Hereto, cardiomyocytes were lysed with 100 µl extraction buffer, incubated on ice for 20 min, and gently resuspended and centrifuged at 10000 x g for 1 min. After protein concentration measurement of the cell lysate, the cell lysate from each group was diluted in extraction buffer to achieve 20 µg protein. 85 µl diluted cell lysate per group was added into each well of a 96-well plate, followed by adding 15 µl master mix (reaction buffer and calpain substrate mixture). After 1 h incubation at 37°C in the dark, the calpain activity was measured

at Ex/Em=390 nm/520 nm. Changes in calpain activity were expressed as relative fluorescent unit (RFU) per μg protein per group.

Fractionation of depolymerized and polymerized α-tubulin

The fractionation of depolymerized and polymerized α-tubulin was described previously for HL-1 cardiomyocytes [4]. After TP, the HL-1 cardiomyocytes were washed with PBS twice, followed by adding the microtubule stabilizing buffer (0.1 M PIPES, 1 mM EGTA, 1 mM $MgCl_2 \cdot 6H_2O$ and 2 M glycerol, pH=6.93) freshly supplemented with (0.5% TritonX-100 and protease inhibition cocktail) to each well on ice for 3 min to extract the soluble α-tubulin, then the remaining cardiomyocytes were washed once with the microtubule stabilizing buffer without supplements, lysed in RIPA buffer containing protease inhibition cocktail, to extract the polymerized α-tubulin fraction, followed by shearing of DNA with an insulin needle and measurement of protein concentration of both fractions by using the Bradford method (Biorad). After the preparation of the fractions, the protein homogenates were used for SDS-PAGE, transferred to the nitrocellulose membranes and incubated with anti-α-tubulin, anti-acetylated α-tubulin, anti-HSPB1 (HSP25) at 4°C overnight and secondary antibodies for 2 h at RT, as described above in the Western blot analysis section.

Immunofluorescent staining and quantification

HL-1 cardiomyocytes were seeded on 0.02% gelatin coated coverslips, followed by TP at 5 Hz for 10 h, and post-treatment with GGA*-59 or chariot rcHSPB1 transfection. Next, HL-1 cardiomyocytes were washed twice with PBS, fixed with 4% paraformaldehyde at RT for 15 min, washed twice with PBS; permeabilized with 0.3% TritonX-100 (in PBS) at RT for 10 min, washed with PBS twice, blocked with blocking solution (0.5% BSA + 0.15% glycine in PBS) at RT for 10 min; incubated with α-tubulin (1:200) and acetylated α-tubulin (1:200) primary antibodies at 4°C overnight, washed with blocking solution 3

times, incubated with anti-rabbit or anti-mouse secondary antibodies at RT in the dark for 1 h; washed with blocking solution at RT for three times, washed with PBS twice, incubated with diluted DAPI (1:500 in PBS) at RT for 30 min, then washed with milliQ water. Finally, the coverslips were sealed with mounting medium, and stored at 4°C at least overnight before microscopic analysis. The images were taken at a DIMI fluorescent microscope by utilizing Slidebook software 6.0. Five to six images per group were chosen for the quantification of the microtubule length. Hereto, the length of 100 α-tubulin and acetylated α-tubulin stained microtubules were measured by using the freehand tool and length measurement function in Image J2.

HDAC6 activity measurement

HL-1 cardiomyocytes were seeded on 0.02% gelatin coated 4-well cell culture plates, followed by subjection to TP at 5 Hz for 10 h, and post-treatment with 10 μM GGA*-59/DMSO or rcHSPB1 for 8 h. After 10 h TP, HL-1 cardiomyocytes were washed with PBS once, and immediately collected in HDAC6 lysis buffer provided within the HDAC6 activity assay kit (BioVision). The other groups were collected after 8 h recovery with or without GGA*-59 or rcHSPB1 post-treatment. The HL-1 cardiomyocytes were incubated with HDAC6 lysis buffer on ice for 5 min, homogenates were centrifuged at 16000 g for 10 min at 4°C. The supernatant was transferred to an empty tube and kept on ice. Protein concentration of each group was measured by using Bradford assay (Biorad). According to the kit instruction, the standard curve was made by diluting AFC fluorophore in HDAC6 assay buffer, to obtain gradient concentrations of AFC (AFC + HDAC6 assay buffer, 100 μl per well in a 96-well plate). Each sample was diluted with HDAC6 assay buffer. HDAC6 substrate mix was prepared from HDAC6 assay buffer and HDAC6 substrate. 50 μl HDAC6 substrate mix was added to 50 μl protein homogenate in each well of a 96-well plate and incubated at 37°C for 30 min in the dark, followed by adding 10 μl developer to each well and incubation at 37°C for 10 min in the dark, to generate the fluorescent signal. The fluorescence was measured at Ex/Em=390 nm/460 nm by fluorometric reader (FLUOstar, BMG

labtechnologies). Changes in HDAC6 activity were calculated as relative fluorescent unit (RFU) per µg/µl protein per sample.

Supplementary Tables

Table S1. Antibodies used for Western blot

Primary antibody	Species	Dilution times
HSPB1 (Hsp25)	rabbit polyclonal	1:1000
HSPB1 (Hsp27)	mouse monoclonal	1:1000
α-tubulin	mouse monoclonal	1:20000
acetylated α-tubulin	mouse monoclonal	1:20000
cTnI	rabbit polyclonal	1:1000
cTnT	mouse monoclonal	1:1000
cTnC	rabbit polyclonal	1:1000
GAPDH	mouse monoclonal	1:5000
β-actin	rabbit polyclonal	1:2000

Table S2. Primers used for quantitative RT-PCR

Gene	Forward primer	Reverse primer
cTnnI3 (mouse)	5’-TCTGCCAACTACCGAGCCTAT-3’	5’-CTCTTCTGCCTCTCGTTCCAT-3’
cTnnT2 (mouse)	5’-CAGAGGAGGCCAACGTAGAAG-3’	5’-CTCCATCGGGGATCTTGGGT-3’
cTnnC1 (mouse)	5’-GCGGTAGAACAGTTGACAGAG-3’	5’-CCAGCTCCTTGGTGCTGAT-3’
Tuba8 (mouse)	5’-CTGAGCAACACCACAGCAAT-3’	5’-CAAACGAATCAGTCCCCACT-3’
Tuba1a (mouse)	5’-GAGCAACACCACAGCCATTG-3’	5’-GGGGCTCAAGGAATGGACTT-3’
Tuba1b (mouse)	5’-CTGATGTATGCCAAGCGTGC-3’	5’-TGGAGCAGTTTGACGACACA-3’
Tuba1c (mouse)	5’-GCATTAACTACCAGCCTCCCA-3’	5’-CCTCACCCTCATCGTCTCCTTC-3’
Tuba4a (mouse)	5’-GGAGGGGACGACTCCTTCA-3’	5’-TGGGCCATTTCGGATCTCATC-3’
β-actin (mouse)	5’-GTGACGTTGACATCCGTAAAGA-3’	5’-GCCGGACTCATCGTACTCC-3’
GAPDH (mouse)	5’-GGGTGTGAACCACGAGAAAT-3’	5’-CCTTCCACAATGCCAAAGTT-3’

Supplementary Figures

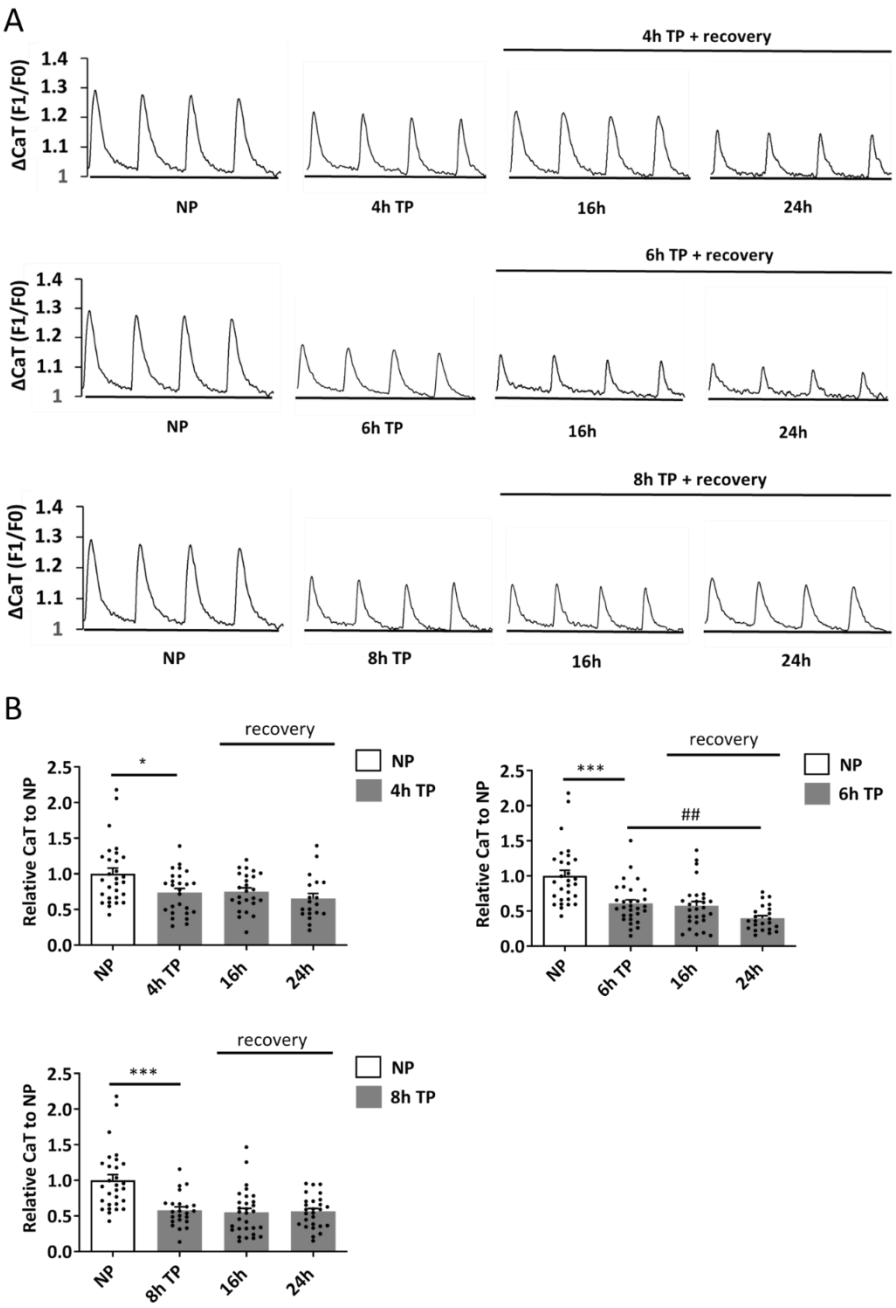

Figure S1. Tachypacing for increasing periods of time results in sustained contractile dysfunction in HL-1 cardiomyocytes

(**A**) Representative CaT of HL-1 cardiomyocytes after non-paced (NP), followed by 4 h, 6 h or 8 h tachypacing (TP), and TP with 16 h or 24 h recovery. (**B**) Quantified CaT amplitudes of HL-1 cardiomyocytes showing 4 h, 6 h and 8 h TP to result in CaT loss, which maintains during 16 h and 24 h recovery. **P*<0.05 and ****P*<0.001 vs NP and $^{\#\#}$*P*<0.01 vs TP. 4h TP+recovery: N (NP)=29, N (4h TP)=26, N (16h)=25, N (24h)=19; 6h TP+recovery: N (NP)=29, N (6h TP)=30, N (16h)=28, N (24h)=23; 8h TP+recovery: N (NP)=29, N (6h TP)=23, N (16h)=30, N (24h)=27.

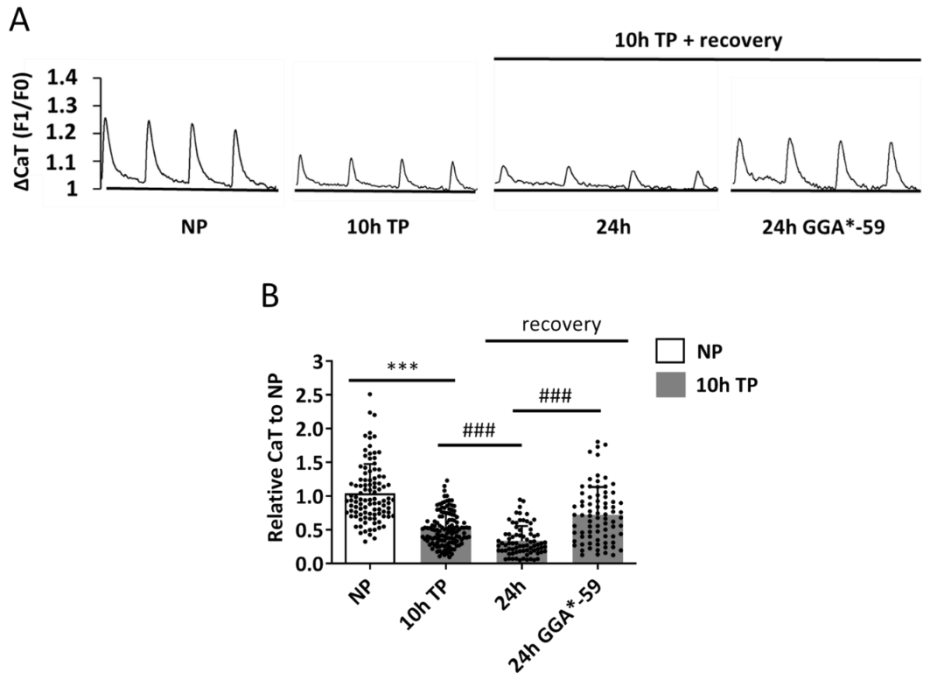

Figure S2. 24 h post-treatment with GGA*-59 restores CaT loss in tachypaced HL-1 cardiomyocytes

(**A**) Representative CaT of non-paced (NP), 10 h tachypacing (TP), TP with 24 h recovery with DMSO post-treatment and TP with 24 h post-treatment with 10 µM GGA*-59 in HL-1 cardiomyocytes. (**B**) Quantified CaT amplitudes of HL-1 cardiomyocytes showing enhanced recovery from CaT loss by 24 h post-treatment with GGA*-59. ****P*<0.001 vs NP and $^{###}P$<0.001 vs 10 h TP or 24 h recovery. N (NP)=101, N (10h TP)=127, N (24h)=76, N (24h GGA*-59)=78.

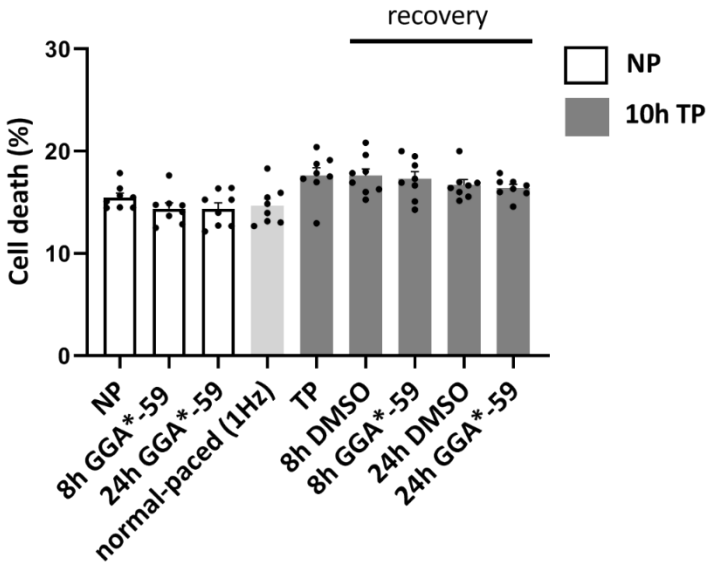

Figure S3. No differences in percentage of cell death in HL-1 cardiomyocytes between the experimental groups

Trypan blue staining shows that the percentage cell death is between 10% and 20% in all the experimental groups. There is no significant difference among non-paced (NP), normal-paced (1Hz), 10 h tachypacing (TP, 5Hz), and TP with 8 h recovery, 24 h recovery and post-treatment with GGA*-59. 57 cardiomyocytes were counted for each group per experiment. Number of independent experiments N=8.

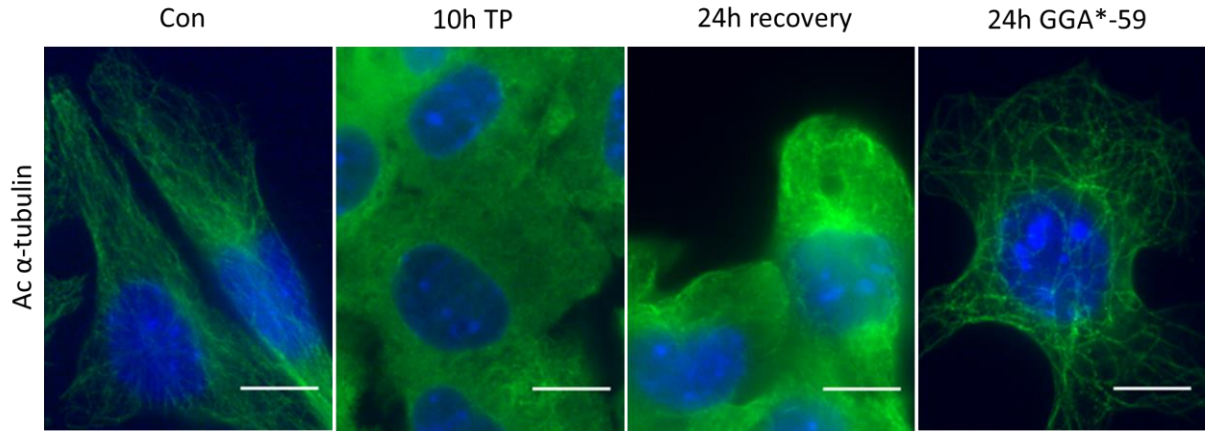

Figure S4. 24h post-treatment of GGA*59 enhances the restoration of the microtubule network

Representative immunofluorescent images showing that the microtubule network in HL-1 cardiomyocytes upon control non-paced (NP), 10 h tachypacing (TP), TP with 24 h recovery with DMSO or GGA*-59 post-treatment. TP results in disruption of the microtubule network which remains disrupted after 24 h recovery, GGA*-59 post-treatment enhances restoration of the microtubule network. The microtubule network is represented by staining of acetylated (Ac) α-tubulin. Scale bars represent 10 µm.

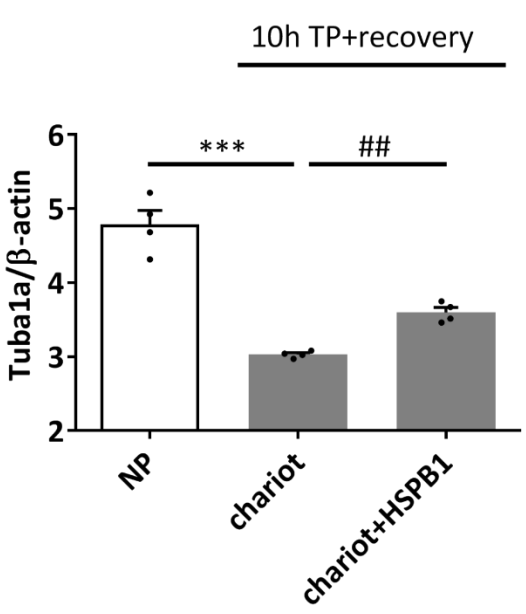

Figure S5. Recombinant HSPB1 upregulates mRNA expression of α-tubulin encoding gene

RT-qPCR data showing 10 h tachypacing (TP) to result in a decrease in mRNA levels of α-tubulin encoding gene *tuba1a*, which maintains decreased during 3 h recovery with chariot reagent, but is significantly increased by post-transfection with rcHSPB1. The mRNA expression level of *tuba1a* is normalized to β-actin. ***P<0.001 vs NP and $^{\#\#}P$<0.01 vs chariot. Number of independent experiments N=3.

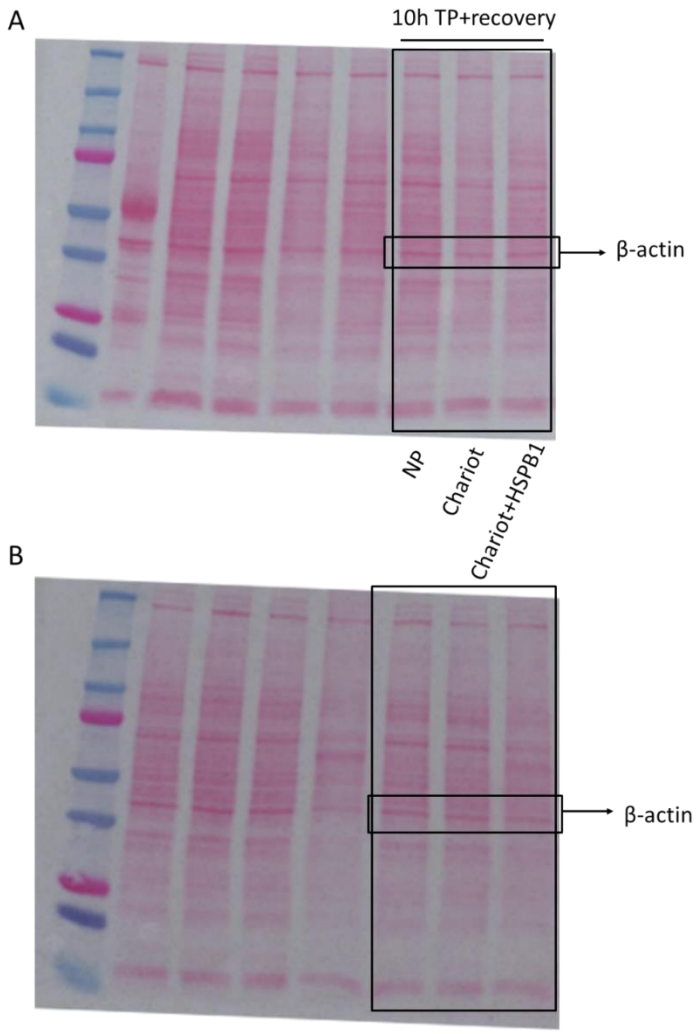

Figure S6. The total protein illustration

The amount of total protein, indicated by the Ponceau S staining, in the chariot HSPB1 transfection experiments. (**A**) The blot includes the experimental groups for detecting the protein expression levels of α-tubulin and acetylated (Ac) α-tubulin, within the bigger black frame. (**B**) The blots includes the experimental groups for detecting the protein expression levels of cTnI, cTnT and cTnC, within the bigger black frame. The smaller black frames specify the bands of β-actin.

References

1. Claycomb WC, et al. HL-1 cells: a cardiac muscle cell line that contracts and retains phenotypic characteristics of the adult cardiomyocyte. Proc Natl Acad Sci U S A. 1998;95:2979-84.
2. Ke L, et al. HSPB1, HSPB6, HSPB7 and HSPB8 protect against RhoA GTPase-induced remodeling in tachypaced atrial myocytes. PloS one. 2011;6:e20395.
3. Paredes RM, et al. Chemical calcium indicators. Methods. 2008;46:143-51.
4. Zhang D, et al. Activation of histone deacetylase-6 induces contractile dysfunction through derailment of alpha-tubulin proteostasis in experimental and human atrial fibrillation. Circulation. 2014;129:346-58.